Two-Point Flux Approximation for Pricing Options under Local Volatility

Richard Mark Mwale (richardmwale@aims.ac.za)
African Institute for Mathematical Sciences (AIMS)

Supervised by: Dr. Hermann Azemtsa Donfack
University of Johannesburg, South Africa
Co-supervised by: Mr. Rock Stephane Koffi
African Institute for Mathematical Sciences, South Africa

22 September 2020
Submitted in partial fulfillment of a structured masters degree at AIMS South Africa

Abstract

In this essay, we present the discretization of the Black-Scholes equation using the finite volume method based on the Two-Point Flux Approximation. We use the method to price European options under local volatility. In Section 2.5 we derived the Black Scholes partial differential equation under local volatility, then in Chapter 3, we use the Two-Point Flux Approximation method to discretize in space, and the Implicit numerical scheme for the time discretization. We compare our results to the well known benchmark methods.

Keywords: Black-Scholes PDE, Option, Local volatility, Two-Point Flux Approximation method (TPFA).

Declaration

I, the undersigned, hereby declare that the work contained in this research project is my original work, and that any work done by others or by myself previously has been acknowledged and referenced accordingly.

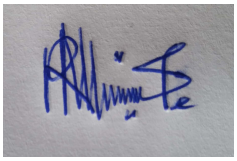

Richard Mwale, 22 September 2020

Contents

1. Introduction

1.1 Background

A financial derivative is an instrument whose value relies on the price of the underlying variable. They can be used to protect against risk, to speculate or to spot arbitrage opportunities (Fernandes, 2009). Options are a popular type of financial derivatives that gives its holder the right but not the obligation to buy (call) or sell (put) an asset on (or before) a fixed date (maturity) for a specified fixed price (strike price) (Hull, 2018). Because of their wide use, pricing options has grown to be a major research area of interest in financial mathematics (Kazeem, 2014). Black and Scholes (1973) proved that the price of an European option can be found by solving the second order parabolic partial differential equation (PDE). They also assumed that the volatility of the underlying asset is known and it is constant, which implies that the volatility of a certain asset would be the same for all strike prices. But in reality, the volatility of an asset changes with time (τ) and strike price (K). In order to get an option value that is closer to that of the market, volatility has to be taken as a function of time and asset price. Many models have been proposed in which the volatility is a function of time and price of the underlying asset, these model include: stochastic volatility model (Hull and White, 1987), jump diffusion models (Merton, 1976) and local volatility (Dupire et al., 1994). Amongst these, the local volatility model is the simplest to implement and fits the market data accurately. Section 2.6 talks more about local volatility model.

Pricing an option with non-constant volatility is considerably more difficult than pricing a similar option with constant volatility. The numerical method used must be able to handle complex diffusion term resulting from the volatility function. For this reason, popular methods such as the finite difference needs to be modified in order to achieve reasonable accuracy. Finite volume methods and finite element methods are often preferred in these conditions.

The upwind method coupled with Two Point Flux Approximation (TPFA) is a type of finite volume method well known in fluid dynamics and has been used in finance to price options (Koffi and Tambue, 2019). Koffi and Tambue (2019) proved the convergence of the solution of the TPFA method. In their paper, they showed the existence and uniqueness of the discretized solution, and they further showed the flux consistency of the method.

1.2 Objective

In this essay, we derive the TPFA method for the Black-Scholes PDE under local volatility, then use it to price a European option. Thereafter we compare the results to other methods contained in the benchmark paper by von Sydow et al. (2015). In this paper, advanced Crank-Nicolson method and some numerical methods were use to price options.

1.3 Outline

The outline of the essay will be as follows: Chapter 2 will talk about the basic notion of finance, in this chapter, we will define some basic concepts that we will need in this study. Chapter 3 will present the numerical methods, this is where we will derive the TPFA method for pricing options under local volatility. Chapter 4 will give the numerical results of the TPFA for a specified problem, and the results

obtained will be compared to those of the benchmark paper. Finally, we present our conclusion in Chapter 5.

2. Preliminaries

In this section, we present some basic concepts, definitions, and notation, which will prove to be useful for better understanding of the topic under study.

2.1 Probability Theory

2.1.1 Definition. A **Sample space** according to Shreve (2004) is defined as a non-empty set of all possible outcomes of an event and is denoted by Ω.

2.1.2 Definition. σ**-Field** (Kloeden and Platen, 1995) A non-empty collection $\mathcal{H}$ of subsets of a sample space Ω is said to be a σ-field if it satisfies the following conditions:

(i) $\Omega \in \mathcal{H}$,

(ii) $\mathcal{B} \in \mathcal{H} \implies \mathcal{B}^c \in \mathcal{H}$, and

(iii) If $(\mathcal{B})_{i\in\mathbb{N}} \in \mathcal{H}$ is a finite sequence, then $\bigcup_{i=0}^{\infty} \mathcal{B}_i \in \mathcal{H}_i$.

The set $(\Omega, \mathcal{H})$ is called a measurable space.

2.1.3 Definition. Probability measure (Durrett, 2019) Suppose $\mathcal{H}$ is a σ-field and Ω a sample space, then the probability measure $\mathbf{P}$ is a real-valued function on $\mathcal{H}$ if the following properties hold:

(i) $\mathbf{P}(\Omega) = 1$,

(ii) $0 \leq \mathbf{P}(\mathcal{B}) \leq 1, \quad \forall \mathcal{B} \in \mathcal{H}$.

(iii) For $\mathcal{B}_1, \mathcal{B}_2, \mathcal{B}_3, \cdots \in \mathcal{H}$ with $\mathcal{B}_i \cap \mathcal{B}_j = \phi, \quad i \neq j$, then

$$\mathbf{P}\left(\bigcup_{i=1}^{\infty} \mathcal{B}_i\right) = \sum_{i=1}^{\infty} \mathbf{P}(\mathcal{B}_i).$$

2.1.4 Definition. Probability space (Durrett, 2019) is defined as the triple space $(\Omega, \mathbf{P}, \mathcal{H})$ having the following properties:

(i) Sample space Ω has all possible outcomes,

(ii) $\mathcal{H}$ contains all events of Ω,

(iii) $\mathbf{P}$ is a probability measure that ranges between 0 and 1.

2.1.5 Definition. Random variable (Shreve, 2004) Let $(\Omega, \mathbf{P}, \mathcal{H})$ be a finite probability space, then a real-valued function defined on a sample space Ω is called a random variable X.

2.2 Stochastic Processes

2.2.1 Definition. Stochastic process (Kloeden and Platen, 1995) A group of random variables on a probability space $(\Omega, \mathbf{P}, \mathcal{H})$, is called a stochastic process given by:

$$S = \{S(t), t \in T\},$$

with $t \in \mathbb{R}$ taken to be time.

2.2.2 Definition. Standard Brownian motion (Kloeden and Platen, 1995) A stochastic process $W = (W_t)_{t\geq 0}$ is said to be a Standard Brownian motion or Wiener process if the following properties hold:

(i) $W = 0$,

(ii) W is a stochastic process with stationary and independent increments,

(iii) $W_t - W_s$ is normally distributed, with $N(0, t-s)$ for $0 \leq s \leq t$.

2.2.3 Definition. Geometric Brownian motion (Ross, 2010) Suppose $\{S = (S_t)_{t\geq 0}\}$is a standard Brownian motion, then a process $\{Z = (Z_t)_{t\geq 0}\}$ defined by:

$$Z(t) = e^{S(t)},$$

is called a geometric Brownian motion.

2.2.4 Definition. Stochastic differential equation (Kloeden and Platen, 1995) A Stochastic Differential Equation (SDE) is an equation which takes the form:

$$dS_t = a(S_t)dt + b(S_t)dW_t,$$

where the functions $a(S_t)$ and $b(S_t)$ are the drift and the volatility (diffusion) respectively, and W_t is a Wiener process.

2.2.5 Lemma. Ito's lemma (Kloeden and Platen, 1995) Let $\{S_t\}$ be a process satisfying

$$dS_t = \mu(S_t)dt + \sigma(S_t)dW_t, \tag{2.2.1}$$

where μ is the drift and σ volatility.

Consider $V(S_t, t)$ to be twice differentiable function of S_t defined in Equation (2.2.1), the SDE followed by $V(S_t, t)$ is given by

$$dV(S_t, t) = \left(\frac{\partial V}{\partial t} + \mu\frac{\partial V}{\partial S} + \frac{\sigma^2}{2}\frac{\partial^2 V}{\partial S^2}\right)dt + \sigma\frac{\partial V}{\partial S}dW_t. \tag{2.2.2}$$

2.3 Financial Terms

2.3.1 Definition. Volatility (Hull, 2018) is defined as a measure of a variation of return of an underlying stock and it is denoted by σ.

2.3.2 Definition. Implied volatility According to Wilmott (2007) implied volatility σ_{imp} is volatility which when put in the Black-Scholes PDE gives an option value which is consistent with the market price.

2.3.3 Definition. Smile (Wilmott, 2007) is defined as the shape caused by the implied volatility σ_{imp} and the strike price K.

2.3.4 Definition. Moneyness (Hull, 2018) is a term that describes the relation between strike price and underlying asset price of the derivative.

2.3.5 Definition. Drift (Hull, 2018) is the average rate of an underlying asset and is denoted by μ.

2.3.6 Definition. Delta (Haug, 2007) is the change in option price divided by the change in the price of the underlying asset, and it is denoted by Δ, mathematically defined as

$$\Delta = \frac{\partial V}{\partial S},$$

where V is the option price and S is the underlying asset price.

2.3.7 Definition. Risk-free rate (Hull, 2018) is the theoretical return rate expected by an investor from their investment without any risk.

2.3.8 Definition. Intrinsic value (Capinski and Zastawniak, 2003) is defined as the measure of an options worth. For instance we have the intrinsic value for a call given by $\max(S-K,0)$ whereas $\max(K-S,0)$ is for put option, where S is the underlying asset price and K is the strike price.

2.3.9 Definition. Extrinsic value is the difference between the market price and the intrinsic value of an option (Capinski and Zastawniak, 2003).

2.3.10 Definition. Time value option (Capinski and Zastawniak, 2003) describes the possibility that an option could increase in value before its expiry date.

2.4 Option Theory

Options are financial derivatives that give its owner the right but not the obligation to buy or sell a stock at a fixed date for a fixed price (Hull, 2018). The main component of an option is that it permits the holder the right to either exercise or to allow it to expire, unlike the forward contract. Generally, options are contracts between two parties which are the buyer and the seller, these two parties can be represented by a bank and an individual, or a bank with another bank or financial institution or even just between two individuals. The buyer of an option assumes a long position whereas the seller assumes a short position (Hull, 2018).

There are numerous types of option styles: American option, European option, Asian option and Barrier option just to mention a few. Amongst these, the most common ones are the American and the European options. The main distinction between American and European options is that, the American option permits the owner to exercise the option at any time during the life of an option, whereas the European option is exercised at the maturity date only (Hull, 2018). There are two kinds of option namely: a call and a put option. According to Hull (2018) a call allows its holder to buy the underlying asset for a fixed price at a specified date and a put allows its owner to sell the underlying asset at a fixed time for a fixed price. The underlying asset can be stocks, property, or a financial instrument just to point out a few. The price at which an asset is agreed to be exercised on is referred to as a strike price or the exercise price and it is denoted by K (Capinski and Zastawniak, 2003). The agreed time at which an option will be exercised is called maturity or the expiration date and it is denoted by T (Capinski and Zastawniak, 2003). The call and put options are connected by a put-call parity theory.

The put-call parity can be used to get the call(put) when given the put(call) price (Haug, 2007). The put-call parity helps to detect the arbitrage opportunities, that is, if the put-call parity does not hold then there exists an arbitrage opportunity (Haug, 2007).

Options can be categorically described into three different behaviour before their expiration date, these are: in the money (ITM), at the money (ATM) and out of the money (OTM) Capinski and Zastawniak (2003). ITM is a term that refers to an option that have intrinsic value. An ITM call option is the one whose underlying asset price S is greater than the strike price K i.e. $S > K$, whereas a ITM put option is the one that has the underlying asset price S is less than the strike price K i.e. $S < K$, in this case, both call and put options are profitable (Lanieri, 2009). The ATM option is one with the same strike price and underlying asset price. Here, the call and put payoffs are the same, i.e $S = K$ (Lanieri, 2009). An OTM option is the one that only contains an extrinsic value, that is, it is a type of an option that does not produce profit if exercised immediately. An OTM call option is one where the underlying asset price (S) is less than the strike price (K), that is $(S < K)$ (Lanieri, 2009). On the other hand, a OTM put option is an option where the underlying asset price (S) is greater than the strike price (K), i.e $(S > K)$ (Lanieri, 2009).

We can summarise the above information using a table. Let K be the strike price with S the underlying asset price at, then we have:

Option Behavior	Call Option	Put Option
ITM	$S > K$	$S < K$
ATM	$S = K$	$S = K$
OTM	$S < K$	$S > K$

Table 2.1: *Behaviour of options before the expiration date*

In this essay, our focus will be on European options. In the above paragraph we stated that, the European option is well known for the ability to be only exercised at the maturity date, unlike American options that can be exercised any time during the life of an option (Hull, 2018). The European payoff is equivalent to the American option payoff if the American option is exercised at the maturity date (Lanieri, 2009). The European option is considered the most simple and easy options to analyse, and is mostly used in the stock and foreign currency and it is cheaper compared to American option (Lanieri, 2009).

Black and Scholes (1973) proved that the price the European option with constant coefficients is obtained by solving a second order Black-Scholes PDE with respect to the underlying asset price and time. But when a European option has no constant coefficient(volatility and drift are changing with time), the Black-Scholes PDE can not be solved analytically to get the price of an option, instead it is solved by using numerical method such as the finite difference method (Courtadon, 1982). The following parameters are needed to value a European option using classical Black-Scholes PDE: the underlying stock price (S), the strike price or exercise price (K), risk-free rate (r), the volatility of an asset (σ), and the maturity (T) (Haug, 2007).

There are two types of European option, these are: European call and put options. The European call allows its holder to buy an asset on the maturity date (Hull, 2018). The payoff of the European call V_{call} option is given by:

$$V_{\text{call}} = \max(S_t - K, 0),$$

where S_t is the asset price at time t.

The payoff of the European call option can be illustrated graphically as shown in Figure 2.1.

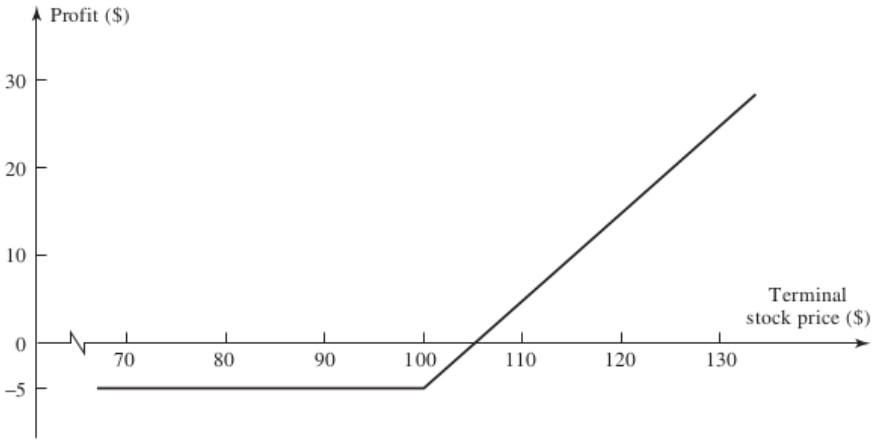

Figure 2.1: *Payoff of the Call option with the option price* $\$5$ *and strike price* $K = \$100$, *Source: (Hull, 2018)*

.

The European put option is defined as an option which permits the holder the right to sell an asset at the maturity (Hull, 2018), and its payoff V_{put} is given by

$$V_{\text{put}} = \max(K - S_t, 0)$$

where S_t is the asset price at time t.

The payoff of the European put can also be can be illustrated graphically as shown in Figure 2.2.

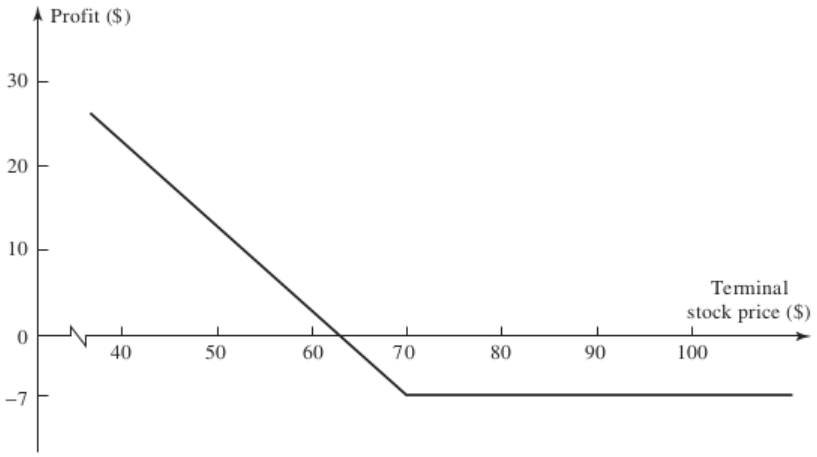

Figure 2.2: *Payoff of the European put on one share of stock with he option price is* $\$7$ *and strike price* $K = \$70$. *Source: (Hull, 2018)*

A European call option can only yield a profit if the strike price (K) is smaller than the underlying asset price (S) as seen in the Figure 2.1, whereas, a European put option can yield a profit if the strike price (K) is larger than the underlying asset price (S) as shown in Figure 2.2.

2.5 Derivation of Black-Scholes PDE

The Black-Scholes PDE is a basic model used for option pricing. This equation is solved analytical to value European options (Ramström, 2017). Here, we will present the derivation of the Black-Scholes PDE under local volatility but before we do that, let us give an outline of the assumptions that Black and Scholes (1973) made to formulate the equation.

(i) Underlying stock follows a geometry Brownian motion.

(ii) No dividends on the underlying asset.

(iii) No transaction costs on the underlying asset.

(iv) No riskless arbitrage opportunities.

(v) Volatility and the risk-free rate of the underlying asset are known and are constant.

With these assumptions above, we use the following notation for our parameters: underlying asset (S), strike price (K), volatility ($\sigma(S,t)$), drift (μ), risk-free rate (r), time to expiry (t) and maturity (T) and option value $V(S,t,\sigma,\mu,K,T,r)$.

Option value can also be written as:

$$V(S,t,\sigma,\mu,K,T,r) \equiv V(S,t),$$

where $\sigma = \sigma(S,t)$.

Suppose Π denote a portfolio of a long option position and a short position in some quantity Δ of the underlying asset S, such that

$$\Pi = V - \Delta S, \tag{2.5.1}$$

where $V = V(S,t)$.

Suppose the underlying asset follows a geometric Brownian motion such as:

$$dS = \mu S dt + \sigma(S,t) S dW, \tag{2.5.2}$$

where dW is a Wiener process such that $dW = \epsilon\sqrt{\Delta t}$ with $\epsilon \sim N(0,1)$.

The value of the portfolio (2.5.1) changes with time, and is given by:

$$d\Pi = dV - \Delta dS. \tag{2.5.3}$$

From Ito's lemma (2.2.2), the change in the underlying asset price is given by:

$$dV = \frac{\partial V}{\partial t}dt + \frac{\partial V}{\partial S}dS + \frac{1}{2}\frac{\partial^2 V}{\partial S^2}dS^2 + \frac{1}{2}\frac{\partial^2 V}{\partial t^2}dt^2 + \frac{\partial^2 V}{\partial t dS}dt dS. \tag{2.5.4}$$

From Equation (2.5.2) we have:

$$dS^2 = \mu^2 S^2 dt^2 + 2\mu\sigma(S,t)S^2 dt dW + \sigma(S,t)^2 S^2 dW^2. \tag{2.5.5}$$

dt is very small such that dt^2 approaches zero that is $dt^2 \approx 0$. Also, we know that $dW = \epsilon\sqrt{dt}$, so we see that $dW^2 = \epsilon dt \approx dt$, and the term $dtdW = dt^2 \approx 0$. With this evaluation, Equation (2.5.5) reduces to

$$dS^2 = \sigma(S,t)^2 S^2 dt. \tag{2.5.6}$$

Multiplying Equation (2.5.2) by dt, we have

$$dtdS = \mu S dt^2 + \sigma(S,t) S dW dt. \tag{2.5.7}$$

Since $dt^2 \approx 0$ and $dWdt \approx 0$, Equation (2.5.7) becomes

$$dtdS = 0. \tag{2.5.8}$$

Inserting Equations (2.5.6) and (2.5.8) into Equation (2.5.4), we get

$$dV = \frac{\partial V}{\partial t}dt + \frac{\partial V}{\partial S}dS + \frac{1}{2}\frac{\partial^2 V}{\partial S^2}\sigma(S,t)^2 S^2 dt \tag{2.5.9}$$

By substituting Equation (2.5.9) into Equation (2.5.3), we get:

$$d\Pi = \frac{\partial V}{\partial t}dt + \frac{1}{2}\frac{\partial^2 V}{\partial S^2}\sigma(S,t)^2 S^2 dt + \frac{\partial V}{\partial S}dS - \Delta dS. \tag{2.5.10}$$

We now eliminate the risk using delta hedging by letting $\Delta = \frac{\partial V}{\partial S}$ so that the risk is reduced to zero. After eliminating the risk ,we get

$$d\Pi = \left(\frac{\partial V}{\partial t} + \frac{1}{2}\sigma(S,t)^2 S^2 \frac{\partial^2 V}{\partial S^2}\right) dt \tag{2.5.11}$$

Equation (2.5.11) is risk-free. We now assume that there is no arbitrage, we have:

$$d\Pi = r\Pi dt, \tag{2.5.12}$$

which we can also write as,

$$d\Pi = r\left(V - S\frac{\partial V}{\partial S}\right)dt. \tag{2.5.13}$$

By substituting (2.5.13) into (2.5.11) we have:

$$r\left(V - S\frac{\partial V}{\partial S}\right)dt = \left(\frac{\partial V}{\partial t} + \frac{1}{2}\sigma(S,t)^2S^2\frac{\partial^2 V}{\partial S^2}\right)dt,$$

$$Vr - rS\frac{\partial V}{\partial S} = \frac{\partial V}{\partial t} + \frac{1}{2}\sigma^2S^2\frac{\partial^2 V}{\partial S^2},$$

$$\frac{\partial V}{\partial t} + \frac{1}{2}\sigma(S,t)^2S^2\frac{\partial^2 V}{\partial S^2} + rS\frac{\partial V}{\partial S} - Vr = 0. \tag{2.5.14}$$

which is called the Black-Scholes PDE.

We have $(S,t) \in \Omega_T = \Omega \times [0,T]$ with $\Omega = (0, S_{\max})$, $\sigma(S,t) > 0$ and $T > 0$, the expiration date; with the following boundary and payoff conditions below

For Call,

$$\begin{cases} V(0,t) = 0 & t \in [0,T], \\ V(S_{\max},t) = S_{\max} - Ke^{-r(T-t)} & t \in [0,T], \\ V(S,T) = \max(S-K,0) & S \in \Omega. \end{cases} \tag{2.5.15}$$

For Put,

$$\begin{cases} V(0,t) = Ke^{-r(T-t)} & t \in [0,T], \\ V(S_{\max},t) = 0 & t \in [0,T], \\ V(S,T) = \max(K-S,0) & S \in \Omega. \end{cases} \tag{2.5.16}$$

2.6 Local Volatility Model

Black and Scholes (1973) assumption of the constant volatility turns out to be invalid. The evidence of this is the implied volatility curve as function of strikes is not flat, it has a shape of the smile. An immediate extension of the Black-Scholes model is to assume that volatility σ is a function of time(t) that is, $\sigma(t)$. Another extension of the volatility of the model is the constant elastic variance (CEV), which assume σ to be a function asset price(S), $\sigma(S)$. But the most popular extension is that of Dupire's which assumes volatility as a function of both asset (S) and time (t).

In this section, we derive the local volatility $\sigma(S,t)$ from market data. Suppose we are given the option prices $C(K,T)$ for all exercise prices K and for all expiration times T, Dupire et al. (1994) showed that if an asset follows the geometric Brownian motion

$$\frac{dS}{S} = rdt + \sigma(S,t)dW_t, \tag{2.6.1}$$

then we can determine the local volatility $\sigma(K,T)$ from a European option value for all K and T, using:

$$\sigma(T,K) = \sqrt{2\left(\frac{C_T + (r-q)KC_K}{K^2 C_{KK}}\right)} \tag{2.6.2}$$

where C_K and C_{KK} are the first and second derivatives of a European call option with respect to the strike price and C_T is the derivative with respect to the maturity date.

Equation (2.6.2) can be written in terms of the implied volatility $\sigma_{imp}(T,K)$, so that we obtain:

$$\sigma(T,K) = \sqrt{\frac{\sigma_{imp}^2 + 2\sigma_{imp}T\left(\frac{\partial\sigma_{imp}}{\partial T} + (r-q)K\frac{\partial\sigma_{imp}}{\partial K}\right)}{1 + 2d_1K\sqrt{T}\frac{\partial\sigma_{imp}}{\partial K} + K^2T\left(d_1d_2\left(\frac{\partial\sigma_{imp}}{\partial K}\right)^2 + \sigma_{imp}\frac{\partial^2\sigma_{imp}}{\partial K^2}\right)}}. \tag{2.6.3}$$

where

$$d_1 = \frac{-\ln(x) + \frac{1}{2}\sigma^2\tau}{\sigma\sqrt{\tau}}, \qquad d_2 = d_1 - \sigma\sqrt{\tau}, \qquad \tau = T - t.$$

We can introduce the change in variable $x = \frac{K}{F(t,T)}$ where $F(t,T)$ is the forward price of the underlying asset and expiry T to eliminate r and q to obtain:

$$\hat{\sigma}(T,x) = \sqrt{\frac{\hat{\sigma}_{imp}^2 + 2\hat{\sigma}_{imp}T\frac{\partial\hat{\sigma}_{imp}}{\partial T}}{1 + 2d_1K\sqrt{T}\frac{\partial\hat{\sigma}_{imp}}{\partial K} + K^2T\left(d_1d_2\left(\frac{\partial\hat{\sigma}_{imp}}{\partial K}\right)^2 + \hat{\sigma}_{imp}\frac{\partial^2\hat{\sigma}_{imp}}{\partial K^2}\right)}} \tag{2.6.4}$$

The full derivation can be found in White (2013).

In order to construct Equation (2.6.4) practically, we need smooth market data, to be able to get the values of C_T, C_K and C_{KK} in this formula. But the market data is not often smooth, this is why smoothing methods are introduced for this purpose (Wilmott, 2007). Constructing local volatility is beyond the scope of this essay, and going forward we will assume that the local volatility function is given by:

$$\sigma(S,t) = 0.15 + 0.15(0.5 + 2t)\frac{\left(\frac{S}{100} - 1.2\right)^2}{\left(\frac{S}{100}\right)^2 + 1.44}, \tag{2.6.5}$$

where S is the asset price and t .

This local volatility function is the same used in the benchmark paper by von Sydow et al. (2015).

3. Discretization of the Black-Scholes Partial Differential Equation (PDE) using TPFA Method under Local Volatility

When volatility is not constant, analytical solutions of the Black-Scholes PDE are difficult to find. In this case, numerical methods are required. Many numerical methods have been developed to solve the Black-Scholes PDE. The most popular are the finite difference method (FDM), the finite element method (FEM) and the finite volume method (FVM). The finite volume method has been extensively used in fluids dynamics. In this essay, we use the finite volume method for the spatial discretization of Black-Scholes PDE. At first we transform the Black-Scholes PDE to its divergence form and integrate each term of the transformed PDE. The TPFA method is used to discretize the integral of the diffusion term and the first order upwind scheme to discretize the integral of the advection term. The other integrals involved in the divergence form of the Black-Scholes PDE are discretized using the mid-point quadrature rule. Afterwards we use the implicit method for the time discretization. In the next sections, we give a detailed derivation of the our approach following the work of Koffi and Tambue (2019). Note that unlike Koffi and Tambue (2019) who used the volatility $\sigma(t)$, in this work the volatility is a function of S and t that is $\sigma(S,t)$.

3.1 Transformation of the Black-Scholes PDE

Before derivation, we need to transform the Black-Scholes equation into its divergence form so that we can easily apply the TPFA method and upwind scheme to the diffusion and advection terms respectively.

We rewrite Equation (2.5.14) as follows;

$$\frac{\partial V}{\partial t} = -\frac{1}{2}\sigma(S,t)^2 S^2 \frac{\partial^2 V}{\partial S^2} - rS\frac{\partial V}{\partial S} + Vr. \tag{3.1.1}$$

Now, using $\tau = T - t$, we have $d\tau = -dt$ so that

$$\frac{\partial V}{\partial \tau} = \frac{1}{2}\sigma(S,\tau)^2 S^2 \frac{\partial^2 V}{\partial S^2} + rS\frac{\partial V}{\partial S} - Vr. \tag{3.1.2}$$

By divergence formulation, we rewrite the equation (3.1.2) to obtain

$$\frac{\partial V}{\partial \tau} = \frac{\partial}{\partial S}\left[aS^2\frac{\partial V}{\partial S} + bVS\right] + cV, \tag{3.1.3}$$

where

$$a = \frac{1}{2}\sigma^2, \quad b = r - \sigma^2 - \sigma_S\sigma S \quad \text{and} \quad c = -2r + \sigma^2 + 4S\sigma_S\sigma + \sigma_{SS}\sigma S^2 + \sigma_S^2 S^2. \tag{3.1.4}$$

Note that: $\sigma^2 = \sigma(S,\tau)^2$ and σ_S, σ_{SS} are the first and the second derivative with respect to S, and $a = a(S,\tau)$, $b = b(S,\tau)$ and $c = c(S,\tau)$.

If the volatility (σ) is constant we have:

$$a = \frac{1}{2}\sigma^2, \quad b = r - \sigma^2 \quad \text{and} \quad c = -2r + \sigma^2. \tag{3.1.5}$$

3.2 Discretization in Space

Let $\Omega = \bigcup_{i=0}^{N-1} \Omega_i$ be a partitioned into sub-intervals such that

$$\Omega_i = [S_i, S_{i+1}] \quad \forall i = 0, \ldots, N, \tag{3.2.1}$$

With $0 = S_1 < S_2 < S_3 < \cdots < S_N < S_{N+1} = S_{\max}$. We define the midpoints of the interval Ω_i as:

$$S_{i-\frac{1}{2}} = \frac{S_{i-1} + S_i}{2} \quad \text{and} \quad S_{i+\frac{1}{2}} = \frac{S_{i+1} + S_i}{2}, \tag{3.2.2}$$

$\forall i = 1, 2, \ldots, N-1$ with $S_{-\frac{1}{2}} = S_0$ and $S_{N-\frac{1}{2}} = S_{\max}$.

Using the above defined midpoints, we can form a second partition J_i of Ω such that

$$J_i = [S_{i-\frac{1}{2}}, S_{i+\frac{1}{2}}]. \tag{3.2.3}$$

3.3 Two-Point Flux Approximation (TPFA) Method

We are now fully equipped to employ the TPFA method to approximate V on the interval J_i. First we let $V(S_i, \tau_j) \approx V_{i,j}$ and $c = c(S_i, \tau_j) \approx c_{i,j}$. By integrating Equation (3.1.3) over J_i we have

$$\int_{J_i} \frac{\partial V}{\partial \tau} dS = \int_{J_i} \frac{\partial}{\partial S}\left[aS^2 \frac{\partial V}{\partial S} + bVS\right] dS + \int_{J_i} cV dS. \tag{3.3.1}$$

Thus

$$\int_{J_i} \frac{\partial V}{\partial \tau} dS = \int_{J_i} \frac{\partial}{\partial S}\left[aS^2 \frac{\partial V}{\partial S}\right] dS + \int_{J_i} \frac{\partial}{\partial S}(bVS) dS + \int_{J_i} cV dS. \tag{3.3.2}$$

By application of midpoint quadrature rule on all the terms in Equation (3.3.2) except for the first and the second terms on the right, we have;

$$\int_{J_i} \frac{\partial V}{\partial \tau} dS \approx l_i \frac{\partial V_{i,j}}{\partial \tau} \quad \text{and} \quad \int_{J_i} cV dS \approx l_i c_{i,j} V_{i,j}. \tag{3.3.3}$$

where $l_i = S_{i+\frac{1}{2}} - S_{i-\frac{1}{2}}$

Thus Equation (3.3.2) becomes

$$l_i \frac{\partial V_{i,j}}{\partial \tau} = \int_{J_i} \frac{\partial}{\partial S}\left[aS^2 \frac{\partial V}{\partial S}\right] dS + \int_{J_i} \frac{\partial}{\partial S}(bVS) dS + l_i c_{i,j} V_{i,j}. \tag{3.3.4}$$

From the first term on the right of Equation (3.3.4), we apply the TPFA method as described by Koffi and Tambue (2019) we have

$$\int_{J_i} \frac{\partial}{\partial S}\left[aS^2\frac{\partial V}{\partial S}\right] dS = aS^2\frac{\partial V}{\partial S}\Big|_{S_{i+\frac{1}{2}}} - aS^2\frac{\partial V}{\partial S}\Big|_{S_{i-\frac{1}{2}}}. \tag{3.3.5}$$

We now define

$$\rho(S) = k(S,\tau)\frac{\partial V}{\partial S} \quad \text{with} \quad k(S,\tau) = a(S,\tau)S^2. \tag{3.3.6}$$

We now approximate ρ over the interval J_i. Thus we first start by replacing $k(S,t)$ by its integral average value that is:

$$k_{i,j} = \frac{1}{l_i}\int_{J_i} a(S,\tau)S^2 dS. \tag{3.3.7}$$

With reference to the Figure 3.1 $\rho_{i+\frac{1}{2}}$ can be evaluated on both the right and left sides of $S_{i+\frac{1}{2}}$

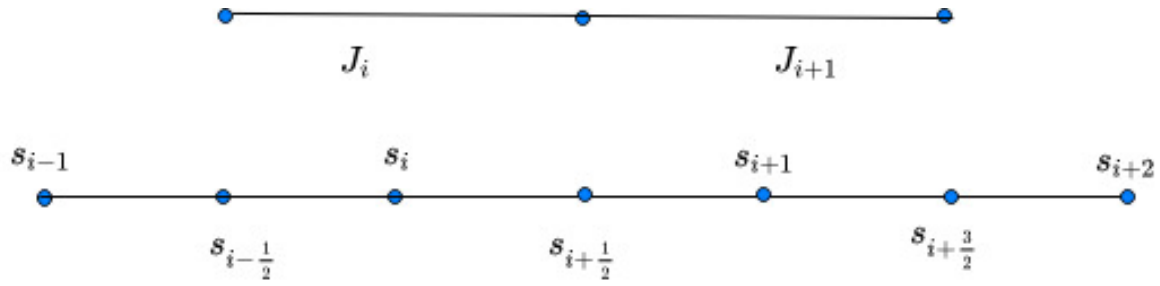

Figure 3.1: Interval subdivision

From Equation (3.3.6), for the left side;

$$\rho_{i+\frac{1}{2},j} = k_{i,j}\frac{V_{i+\frac{1}{2},j} - V_{i,j}}{\frac{l_i}{2}} = 2k_{i,j}\frac{V_{i+\frac{1}{2},j} - V_{i,j}}{l_i}. \tag{3.3.8}$$

Similarly for the right hand side

$$\rho_{i+\frac{1}{2},j} = k_{i+1,j}\frac{V_{i+1,j} - V_{i+\frac{1}{2},j}}{\frac{l_{i+1}}{2}} = 2k_{i+1,j}\frac{V_{i+1,j} - V_{i+\frac{1}{2},j}}{l_{i+1}}. \tag{3.3.9}$$

By using the continuity flux at the interface $S_{i+\frac{1}{2}}$, we equate the Equations (3.3.8) and (3.3.9) to obtain

$$V_{i+\frac{1}{2},j} = \frac{\frac{k_{i,j}}{l_i}V_{i,j} + \frac{k_{i+1,j}}{l_{i+1}}V_{i+1,j}}{\frac{k_{i,j}}{l_i} + \frac{k_{i+1,j}}{l_{i+1}}}. \tag{3.3.10}$$

then rewrite $\rho_{i+\frac{1}{2},j}$ in Equation (3.3.8) and (3.3.9) by letting $\nu_{i,j} = \frac{k_{i,j}}{l_i}$ to get:

$$\rho_{i+\frac{1}{2},j} = \lambda_{i+\frac{1}{2},j}(V_{i+1,j} - V_{i,j}) \quad \text{with} \quad \lambda_{i+\frac{1}{2},j} = \frac{2\nu_{i,j}\nu_{i+1,j}}{\nu_{i,j} + \nu_{i+1,j}}. \tag{3.3.11}$$

Now to approximate the second term on the right of Equation (3.3.4), we employ the upwind scheme, that is:

$$\int_{J_i} \frac{\partial}{\partial S}(bVS)\, dS = bsV \Big|_{S_{i-\frac{1}{2}}}^{S_{i+\frac{1}{2}}} \approx b\left(S_{i+\frac{1}{2}}V_{i+\frac{1}{2},j} - S_{i-\frac{1}{2}}V_{i-\frac{1}{2},j}\right). \tag{3.3.12}$$

Using Figure 3.1 we have:

$$V_{i+\frac{1}{2},j} = \begin{cases} V_{i,j}, & \text{if} \quad b > 0 \\ V_{i+1,j}, & \text{if} \quad b < 0 \end{cases} \tag{3.3.13}$$

Writing in compact form, we have:

$$bS_{i+\frac{1}{2}}V_{i+\frac{1}{2},j} = S_{i+\frac{1}{2}}V_{i,j}\max(b,0) + S_{i+\frac{1}{2}}V_{i+1,j}\min(b,0), \tag{3.3.14}$$

for $S_{i+\frac{1}{2}} > 0$.

Similarly using Figure 3.1 again, we have:

$$V_{i-\frac{1}{2},j} = \begin{cases} V_{i-1,j}, & \text{if} \quad b > 0 \\ V_{i,j}, & \text{if} \quad b < 0 \end{cases} \tag{3.3.15}$$

Thus for $S_{i-\frac{1}{2}} > 0$, we have:

$$bS_{i-\frac{1}{2}}V_{i-\frac{1}{2},j} = S_{i-\frac{1}{2}}V_{i-1,j}\max(b,0) + S_{i-\frac{1}{2}}V_{i,j}\min(b,0). \tag{3.3.16}$$

By substituting Equations (3.3.11), (3.3.14) and (3.3.16) in Equation (3.3.4) so that the discretization in space is given by:

$$l_i \frac{dV_{i,j}}{d\tau} = F\left(V_{i+\frac{1}{2},j}\right) - F\left(V_{i-\frac{1}{2},j}\right) + l_i c_{i,j} V_{i,j}, \tag{3.3.17}$$

where

$$F\left(V_{i+\frac{1}{2},j}\right) = \lambda_{i+\frac{1}{2},j}\left(V_{i+1,j} - V_{i,j}\right) + S_{i+\frac{1}{2}} V_{i,j} \max\left(b,0\right) + S_{i+\frac{1}{2}} V_{i+1,j} \min\left(b,0\right), \tag{3.3.18}$$

and

$$F\left(V_{i-\frac{1}{2},j}\right) = \lambda_{i-\frac{1}{2},j}\left(V_{i,j} - V_{i-1,j}\right) + S_{i-\frac{1}{2}} V_{i-1,j} \max\left(b,0\right) + S_{i-\frac{1}{2}} V_{i,j} \min\left(b,0\right). \tag{3.3.19}$$

By substituting Equations (3.3.18) and (3.3.19) into (3.3.17) and simplifying we obtain

$$l_i \frac{dV_{i,j}}{d\tau} = \xi_{i,j} V_{i-1,j} + \phi_{i,j} V_{i,j} + \psi_{i,j} V_{i+1,j} \tag{3.3.20}$$

where

$$\xi_{i,j} = \lambda_{i-\frac{1}{2},j} - S_{i-\frac{1}{2}} \max\left(b,0\right), \tag{3.3.21}$$

$$\phi_{i,j} = -\lambda_{i+\frac{1}{2},j} + S_{i+\frac{1}{2}} \max\left(b,0\right) - \lambda_{i-\frac{1}{2},j} - S_{i-\frac{1}{2}} \min\left(b,0\right) + l_i c_{i,j}, \tag{3.3.22}$$

$$\text{and} \quad \psi_{i,j} = \lambda_{i+\frac{1}{2},j} + S_{i+\frac{1}{2}} \min\left(b,0\right), \tag{3.3.23}$$

for $1 \leq i \leq N-1$ and $0 \leq j \leq M$.

We can write equation (3.3.20) into the following matrix form by applying the boundary conditions (2.5.15) and (2.5.16):

$$L\frac{dV}{d\tau} = CV + D, \tag{3.3.24}$$

where

$$L = \begin{bmatrix} l_1 & 0 & 0 & . & . & 0 \\ 0 & l_2 & 0 & . & . & 0 \\ 0 & 0 & l_3 & . & . & 0 \\ . & . & . & . & . & . \\ . & . & . & . & . & . \\ . & . & . & 0 & l_{N-2} & 0 \\ . & . & . & 0 & 0 & l_{N-1} \end{bmatrix}, C = \begin{bmatrix} \phi_{1,j} & \psi_{1,j} & 0 & . & . & 0 \\ \xi_{2,j} & \phi_{2,j} & \psi_{1,j} & . & . & . \\ . & . & . & . & . & . \\ . & . & . & . & . & . \\ . & . & . & . & . & . \\ . & . & . & \xi_{N-2,j} & \phi_{N-2,j} & \psi_{N-2,j} \\ 0 & . & . & 0 & \xi_{N-1,j} & \phi_{N-1,j} \end{bmatrix}$$

$$V = \begin{bmatrix} V_{1,j} \\ V_{2,j} \\ . \\ . \\ . \\ V_{N-2,j} \\ V_{N-1,j} \end{bmatrix} \quad \text{and} \quad D = \begin{bmatrix} V_{0,j}\xi_{1,j} \\ 0 \\ . \\ . \\ . \\ 0 \\ \psi_{N-1,j} V_{N,j} \end{bmatrix}.$$

From Equation (3.3.24) we further simplify to get

$$\frac{dV}{d\tau} = AV + B, \tag{3.3.25}$$

where $A = L^{-1}C$ and $B = L^{-1}D$.

3.4 Discretization in Time

We now discretize Equation (3.3.25), by letting τ_i be in $[0, T]$ such that we have $0 < \tau_1 < \tau_2 < \tau_3 < \cdots < \tau_M = T$ where M is a positive integer and $\Delta\tau = \tau_{n+1} - \tau_n$ with $\Delta\tau \geq 0$ is positive. By applying the fully implicit scheme to equation (3.3.25) we have;

$$\frac{V^{j+1} - V^j}{\Delta\tau} = A^{j+1}V^{j+1} + B^{j+1},$$

$$V^{j+1} - V^j = \Delta\tau \left(A^{j+1}V^{j+1} + B^{j+1}\right),$$

$$V^j = (I - \Delta\tau A^{j+1})V^{j+1} - \Delta\tau B^{j+1},$$

$$V^{j+1} = (I - \Delta\tau A^{j+1})^{-1}(V^j + \Delta\tau B^{j+1}), \tag{3.4.1}$$

where I is an identity matrix of size $N - 1$ with $0 \leq j \leq M$.

4. Numerical Computations and Results

In this chapter we price the European call option using TPFA method derived in Chapter 3. We compare the results we obtain to that of benchmark paper. The benchmark results of Problem 3 of the paper by von Sydow et al. (2015) were computed using advanced Crank-Nicolson methods and other numerical methods. But before we implement the TPFA method under local volatility. We first consider the case where the volatility is constant. This will allows us to find optimal values of N_s (number of discretization points in the asset axis) and M_t (number of discretization points in the times axis). This case is significant because there exists an analytical solution that we can reliably compare our results to.

4.1 Implementation

All codes were run using Python 3.7.3 programming language, and below we present the steps or phases in the implementation process.

Step 1: Definition of the parameters that will be used in the code.

N_s, M_t, $S_{\max}$ (maximum stock price), K (strike price), T (maturity), $S = [0, S_{\max}]$ space discretization, $\tau = [0, T]$ (time discretization), r (risk-free interest rate) $dS = \frac{S_{\max}}{N}$ (asset step size), and $d\tau = \frac{T}{M}$ (time step size).

Step 2: Definition of the local volatility function given by Equation (2.6.5), and its first and second derivatives.

Algorithm 1: Local volatility.

def localvol(S, t):
    return $\sigma(S, \tau)$
def localvol$'(S, \tau)$:
    return $\sigma'(S, \tau)$
def localvol$''$ (S,τ):
    return $\sigma''(S, \tau)$

Step 3: Computation of the coefficients a, b and c from Equation (3.1.4).

Algorithm 2: Coefficients a, b and c

Initialize a, b and c:
a=zeros$[N_s + 1, M_t + 1]$
b=zeros$[N_s + 1, M_t + 1]$
c=zeros$[N_s + 1, M_t + 1]$
for i in$[0, N_s]$:
    for j in $[0, M_t]$:
        do a$_{i,j} = \frac{1}{2}\sigma^2(S_i, \tau_j)$
        do b$_{i,j} = r - \sigma^2(S_i, \tau_j) - \sigma_S(S_i, \tau_j)\sigma(S_i, \tau_j)S$
        do c$_{i,j} = -2r + 4S_i\sigma_S(S_i, \tau_j)\sigma(S, \tau_j) + \sigma_{SS}(S, \tau_j)\sigma(S, \tau_j)S_i^2 + \sigma_S^2(S_i, \tau_j)S_i^2$
    end
end

Step 4:Construction of the interval J_i, which is given by Equation (3.2.3).

Algorithm 3: Interval J_i.

L=[ ]
for i in $[0, N_s]$:
    do L.append$\left(\frac{S_{i+1}-S_i}{2}\right)$
J= array(L)
J = insert(J,0,0)
J = insert(J,$N_s+1, S_{\max}$)
$l_i = \frac{J[N_s-2]-J[1]}{N_s-1}$

Step 4: Computation of k_{ij} and lambda ($\lambda_{i,j}$), since we have our interval J_i and the local volatility function, then we can easily compute k_{ij} thereafter we find $\lambda_{i,j}$ using Equations (3.3.7) and (3.3.11) respectively.

Algorithm 4: Computation of k_{ij} and $\lambda_{i,j}$.

k_{ij} = zeros(N_s+1, M_t+1)
for i in [0,N_s]:
    for j in [0,M_t]:
        do $k_{i,j} = \frac{1}{l_1}\int_{J_i}\frac{1}{2}\sigma^2(S_i,\tau_j)S^2dS$
    end
end
λ_{ij} = zeros(N_s, M_t+1)
for i in [0,N_s-1]:
    for j in [0,M_t]:
        do $\lambda_{i,j} = \frac{2k_{i,j}k_{i,j+1}}{l_{i+1}k_{i,j}+l_ik_{i,j+1}}$
    end
end

Step 5: Computation of $\xi_{i,j}, \phi_{i,j}$ and $\psi_{i,j}$, having done the previous steps, we can now calculate our $\xi_{i,j}, \phi_{i,j}$ and $\psi_{i,j}$ using Equations (3.3.21), (3.3.22) and (3.3.23) respectively.

Algorithm 5: Computation of $\xi_{i,j}, \phi_{i,j}$ and $\psi_{i,j}$.

Initialise ξ, ϕ and ψ
$\xi_{i,j}$ = zeros(N_s-1, M_t)
$\phi_{i,j}$ = zeros(N_s-1, M_t)
$\psi_{i,j}$ = zeros(N_s-1, M_t)
for i in [0,N_s-1]:
    for j in [0,M_s]:
        do $\xi_{i,j} = \lambda_{i,j} - J_i\max(b_{i,j}, 0)$
        do $\phi_{i,j} = -\lambda_{i+1,j} + J_{i+1}\max(b_{i,j},0) - \lambda_{i,j} - J_i\min(b_{i,j},0) + l_ic_{i,j}$
        do $\psi_{i,j} = \lambda_{i+1,j} + J_{i+1}\min(b_{i,j},0)$
    end
end

Step 6: Construction of the grid and computation of the matrices A and B. We can now use Equation (3.4.1) to find the option price at each internal node in the grid by using LU decomposition method to

solve the system of equations of the form $Ax = B$.

Algorithm 6: Construction of the grid and computation of the matrices A and B.

Initialise the grid: grid $=$ zeros$(N_s + 1, M_t + 1)$
Implement the boundary conditions.
grid$[:, 0] = \max(S - K, 0)$
grid$[N_s, :] = S_{\max} - Ke^{-r\tau}$ at $S = S_{\max}$
grid$[0, :] = 0$ at $S = 0$
Construction of the matrices A and B.
Initialise B: B=zeros$(N_s - 1)$
Define the identity matrix I $=$ eye(N_s-1)
for j in $[0, M_t - 1]$:
do
$A = l^{-1}$ (diag$(\phi[0 : N_s - 1, j + 1])$ + diag$(\psi[0 : N - 2, j + 1])$ + diag$(\xi[1 : N_s - 1, j + 1])$)
$B[-1] = l^{-1}$ $(\psi[N_s - 2, j + 1]$grid$[N_s, j + 1])$
Amatrix $= (I - d\tau$A$)^{-1}$
Bvector= grid$[1 : N_s, j] + d\tau B$
Amatrix=LU
Solving a system of equation using LU decomposition method
sol$_1$=solve(L,Bvector)
sol$_2$=solve(U,sol$_1$)
grid$[1 : N_s j + 1]$ =sol$_2$

The final step in the implementation is interpolation to get the option price at any desired asset price, this can be achieved as follows:

$$\text{price} = \text{interp}\,(S0, S, \text{grid}[:, M_t]) \tag{4.1.1}$$

where S0 is the asset price at which we want to value an option.

4.2 Case Study 1: Results

In this section we present the results of the TPFA method under constant volatility. We observe how the values N_s and M_t affect the accuracy of the TPFA method.

4.2.1 Effects of the values of Ns and Mt on the option prices.

We implement the steps presented in Section 4.1, by using the grid $\Omega = (0, S_{\max}) \times (0, T)$, $S_{\max} = 300$, $K = 100$, $r = 0.03$, and taking volatility to be $\sigma = 0.15$ as in Problem 1 of von Sydow et al. (2015). For the TPFA method we choose $Ns \in [100, 2000]$ and $Mt \in [100, 1000]$. We calculate the relative error given by:

$$\text{Error} = \left| \frac{p - p^{ref}}{p^{ref}} \right| \tag{4.2.1}$$

Where p is the option value in the table and p^{ref} is the benchmark call price. We summarise our result in the following relative error plots in Figure 4.1

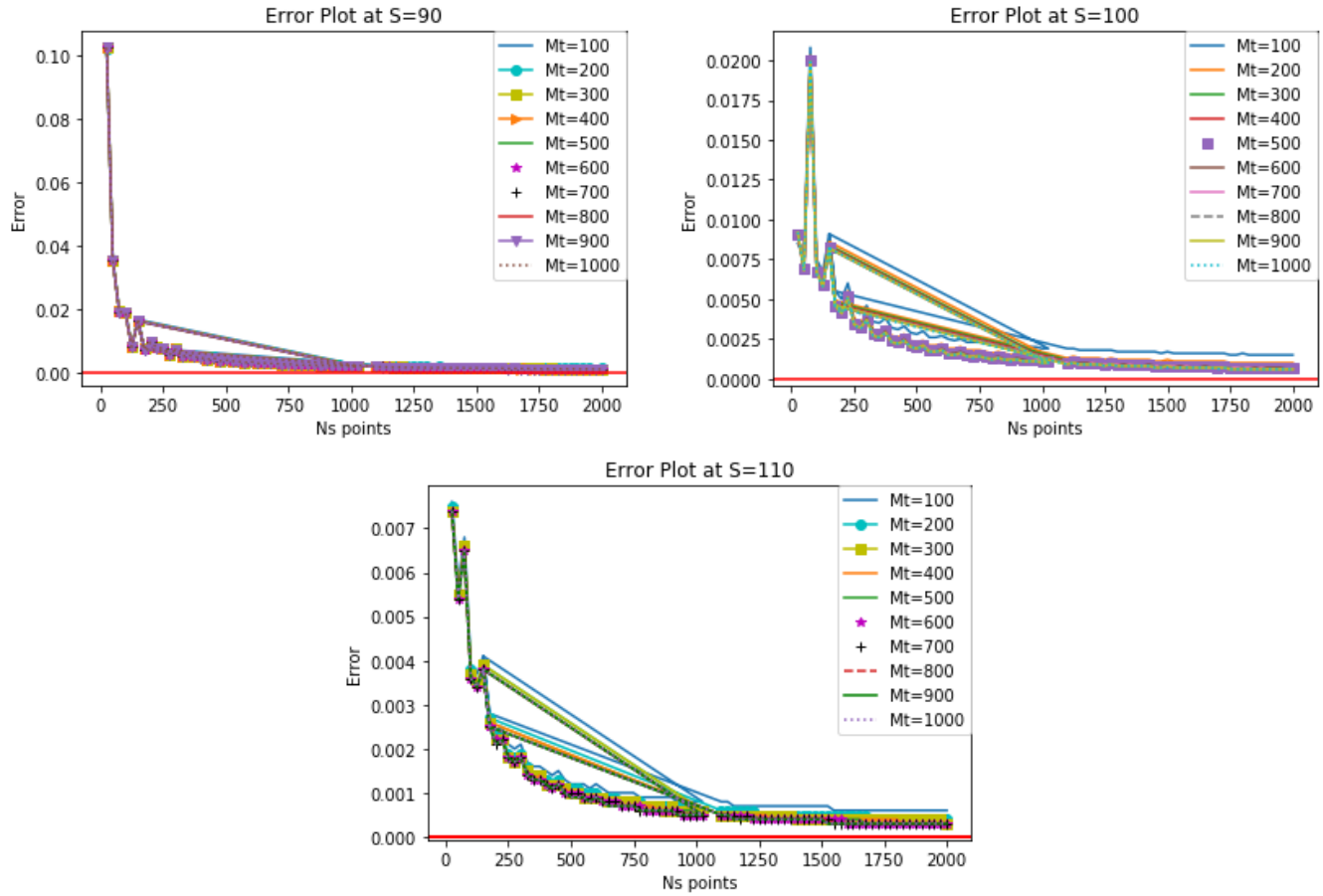

Figure 4.1: European call option relative error plots for different grid sizes at different asset prices, top left at $S0 = 90$, top right at $S0 = 100$ and bottom at $S0 = 110$.

In Figure 4.1, we observe that from the graphs, the relative error decreases as the number of N_s gets larger. We also observe that the value of M_t has minimal effect on the relative error. Furthermore we see that for $N_s \geq 1000$, graphs flatten as they approach zero. This suggests that the TPFA method begins to converge at $N_s = 1000$.

We focus on the region $N_s \in [1000, 2000]$ and $M_t \in [200, 800]$. We study the changes in the option price and their corresponding errors.

Constant volatility option prices at $S0 = 90$				
Ref option price =2.75844				
Ns xMt	200	400	600	800
1000	2,7524	2,7528	2,7529	2,753
1200	2,7531	2,7535	2,7536	2,7537
1400	2,7539	2,7543	2,7544	2,7545
1600	2,7543	2,7547	2,7549	2,755
1800	2,7546	2,755	2,7552	2,7552
2000	2,755	2,7554	2,7555	2,7556

Table 4.1: *TPFA constant volatility option prices at $S0 = 90$ for different grid size. We see that N_s has more effect on the option price than M_t, so as the N_s gets larger the option price get closer to the option price of the benchmark results, which is 2.7584 in this case.*

Constant volatility prices at $S0 = 100$				
Ref option price =7.4851				
Ns x Mt	200	400	600	800
1000	7,4744	7,4763	7,477	7,4773
1200	7,4752	7,4771	7,4777	7,4781
1400	7,4763	7,4783	7,4789	7,4792
1600	7,477	7,4789	7,4795	7,4798
1800	7,4773	7,4792	7,4798	7,4801
2000	7,4778	7,4797	7,4803	7,4807

Table 4.2: *TPFA constant volatility option prices at $S0 = 100$ for different grid size. We see that N_s has more effect on the option price than M_t, so as the N_s gets larger the option price get closer to the option price of the benchmark results given by 7.4850.*

Constant volatility option prices at $S0 = 110$				
Ref option price =14.7020				
Ns x Mt	200	400	600	800
1000	14,6927	14,694	14,6944	14,6946
1200	14,6936	14,6948	14,6952	14,6955
1400	14,6946	14,6959	14,6963	14,6965
1600	14,6952	14,6965	14,6969	14,6971
1800	14,6956	14,6968	14,6973	14,6975
2000	14,696	14,6973	14,6977	14,6979

Table 4.3: *TPFA constant volatility option prices at $S0 = 110$ for different grid size. We see that N_s has more effect on the option price than M_t, so as the N_s gets larger the option price get closer to the option price of the benchmark results, given by 14.7020.*

Tables 4.1, 4.2 and 4.3 contains the relative errors at spot $S0 = 90$, $S0 = 100$ and $S0 = 110$ respectively.

Relative error at $S0 = 90$				
Ns x Mt	200	400	600	800
1000	2,2E-3	2,1E-3	2,0E-3	2,0E-3
1200	1,9E-3	1,8E-3	1,7E-3	1,7E-3
1400	1,7E-3	1,5E-3	1,5E-3	1,4E-3
1600	1,5E-3	1,3E-3	1,3E-3	1,3E-3
1800	1,4E-3	1,2E-3	1,2E-3	1,2E-3
2000	1,3E-3	1,1E-3	1,1E-3	1,0E-3

Table 4.4: *Relative error at $S0 = 90$, as we mentioned in the above paragraph we observe from this table that TPFA method begins to converge at $N_s = 1000$, and as we increase N_s, the relative error tends to get smaller, as small as 10^{-3}.*

Relative error at $S0 = 100$				
Ns xMt	**200**	**400**	**600**	**800**
1000	1,4E-3	1,2E-3	1,1E-3	1,0E-3
1200	1,3E-3	1,1E-3	1.0E-3	9,02E-4
1400	1,2E-3	9,0E-4	8.0E-4	8.0E-4
1600	1,1E-3	8.0E-4	7.0E-4	7.0E-4
1800	1.0E-3	8.0E-4	7.0E-4	7.0E-4
2000	1.0E-3	7.0E-4	6.0E-4	6.0E-4

Table 4.5: *Relative error in option prices at $S0 = 100$, the behaviour of option prices with reference to the relative errors in the table is similar to the one in Table 4.4, which is 10^{-4}.*

Relative error at $S0 = 110$				
Ns x Mt	**200**	**400**	**600**	**800**
1000	6.0E-4	5.0E-4	5.0E-4	5.0E-4
1200	6.0E-4	5.0E-4	5.0E-4	4.0E-4
1400	5.0E-4	4.0E-4	4.0E-4	4.0E-4
1600	5.0E-4	4.0E-4	3.0E-4	3.0E-4
1800	4.0E-4	4.0E-4	3.0E-4	3.0E-4
2000	4.0E-4	3.0E-4	3.0E-4	3.0E-4

Table 4.6: *Showing the Relative error at $S0 = 110$,and it show same pattern as those in Table 4.10 and Table 4.11.But for this case we observe that at $N_s = 1000$ we have the error of 10^{-4}, which means that at $S = 110$, the TPFA method converges fast and attains a relative error of 10^{-4}.*

Tables 4.1, 4.2 and 4.3 contains the option prices at $S0 = 90$, $S0 = 100$ and $S0 = 110$ respectively for different grid sizes. We noticed that the value of an option converges as we increase the grid size. As seen in Figure 4.1 that for $N_s \geq 1000$ all the plots approaches zero, this confirm the convergence of the TPFA method. The maximum error of the TPFA method of the three spot price is in the order of 10^{-3}.

Figure 4.2 shows the relative error obtained by different methods from the benchmark results.

Table 4. Problems 2 and 3. Computational time to compute a solution u that has a relative error $< 10^{-4}$ at $t = 0$ and $s = 90, 100, 110$.

	Discrete dividends				Local volatility			
Method	European call		American call		Smooth		Implied	
MC-S	*6.0e+01	(3)	–		×		×	
QMC-S	1.6e+00	(4)	–		–		–	
FFT	1.5e−03	(7)	–		–		–	
FGL	3.6e−03	(14)	8.1e−02	(6)	–		–	
COS	8.8e−04	(5)	2.4e−03	(4)	1.7e−02	(4)	–	
FD	2.0e−02	(4)	1.5e−02	(4)	2.2e−02	(4)	1.2e+00	(4)
FD-NU	1.6e−02	(4)	1.5e−02	(4)	3.7e−02	(4)	8.9e−01	(4)
FD-AD	2.1e−02	(4)	2.3e−02	(5)	3.6e−02	(4)	8.8e−01	(4)
RBF	2.3e−01	(4)	1.1e−01	(4)	5.5e−02	(4)	2.4e+00	(4)
RBF-FD	4.2e−01	(4)	2.7e+00	(4)	2.2e+01	(4)	1.1e+02	(4)
RBF-PUM	3.3e−02	(4)	3.0e−02	(4)	1.4e−01	(4)	9.0e−01	(4)
RBF-LSML	5.0e−01	(4)	1.2e+00	(4)	1.7e−01	(4)	4.0e+00	(4)

Note: The numbers within parentheses indicate the approximate number of correct digits in the result. A ' – ' indicates not implemented, while ' × ' means implemented, but not accurate.

Figure 4.2: Table of relative error obtained by using different numerical methods. Source : (von Sydow et al., 2015).

Figure 4.2 is a screenshot of the errors in Problem 3 of the benchmark paper, The highlighted region shows the errors obtained by different types of numerical methods. As seen from the errors obtained by all Finite difference methods (FD, FD-NU, FD-AD) is of order 10^{-2} which is higher compared to 10^{-3} obtained by the TPFA.

4.3 Case Study 2: Results

In this section we price a European option under local volatility. We use the parameter of problem of the benchmark paper. Where the volatility is given by Equation (2.6.5). We use $N_s \in [1000, 2000]$ and $M_t \in [200, 800]$. We obtain the following tables.

TPFA local volatility option prices at $S0 = 90$				
with Benchop price =2.955217				
Ns x Mt	**200**	**400**	**600**	**800**
1000	3,035	3,0349	3,0349	3,0349
1200	3,0357	3,0356	3,0356	3,0356
1400	3,0365	3,0364	3,0364	3,0363
1600	3,0369	3,0369	3,0368	3,0368
1800	3,0372	3,0371	3,0371	3,0371
2000	3,0376	3,0375	3,0375	3,0375

Table 4.7: *TPFA local volatility option prices at $S0 = 90$, and we observe that the value of the option converges to the value 3.037 as the grid size gets larger.*

TPFA local volatility option prices at $S0 = 100$ with Benchop price = 7.64217				
Ns x Mt	200	400	600	800
1000	7,8085	7,8095	7,8098	7,81
1200	7,8089	7,8099	7,8102	7,8104
1400	7,8098	7,8108	7,8111	7,8113
1600	7,8102	7,8112	7,8115	7,8117
1800	7,8104	7,8114	7,8117	7,8118
2000	7,8108	7,8118	7,8121	7,8123

Table 4.8: *TPFA local volatility option prices at $S0 = 100$ for different grid size, we see from the that the option price converges to the value 7.812 as we increase the grid size.*

TPFA local volatility option prices at $S0 = 110$ with Benchop price = 14.78425				
Ns x Mt	200	400	600	800
1000	15,2326	15,2323	15,2322	15,2321
1200	15,2326	15,2323	15,2322	15,2321
1400	15,233	15,2327	15,2326	15,2326
1600	15,2332	15,2329	15,2328	15,2327
1800	15,2332	15,2329	15,2328	15,2327
2000	15,2334	15,2331	15,233	15,233

Table 4.9: *TPFA local volatility option prices at $S0 = 110$ for different grid size, we see the that the option price converges to the value 15.233 as the grid size gets larger.*

Relative error at $S0 = 90$				
Ns x Mt	200	400	600	800
1000	2,63E-02	2,63E-02	2,62E-02	2,62E-02
1200	2,65E-02	2,65E-02	2,65E-02	2,65E-02
1400	2,68E-02	2,67E-02	2,67E-02	2,67E-02
1600	2,69E-02	2,69E-02	2,69E-02	2,69E-02
1800	2,70E-02	2,70E-02	2,70E-02	2,70E-02
2000	2,71E-02	2,71E-02	2,71E-02	2,71E-02

Table 4.10: *Relative error in the option prices at $S0 = 90$ for different grid size calculated in Table 4.7, and from the table we see that the error converges to 10^{-2} with increase in grid size.*

Relative error at $S0 = 100$				
Ns x Mt	200	400	600	800
1000	2,13E-02	2,14E-02	2,15E-02	2,15E-02
1200	2,14E-02	2,15E-02	2,15E-02	2,15E-02
1400	2,15E-02	2,16E-02	2,16E-02	2,16E-02
1600	2,15E-02	2,16E-02	2,17E-02	2,17E-02
1800	2,15E-02	2,17E-02	2,17E-02	2,17E-02
2000	2,16E-02	2,17E-02	2,18E-02	2,18E-02

Table 4.11: *Relative error in the option prices at $S0 = 100$ for different grid size calculated in Table 4.8, and the error converges to 10^{-2} as we increase the size of the grid.*

Relative error at $S0 = 110$				
Ns x Mt	**200**	**400**	**600**	**800**
1000	2,94E-02	2,94E-02	2,94E-02	2,94E-02
1200	2,94E-02	2,94E-02	2,94E-02	2,94E-02
1400	2,95E-02	2,94E-02	2,94E-02	2,94E-02
1600	2,95E-02	2,95E-02	2,94E-02	2,94E-02
1800	2,95E-02	2,95E-02	2,94E-02	2,94E-02
2000	2,95E-02	2,95E-02	2,95E-02	2,95E-02

Table 4.12: *Relative error in the option prices at $S0 = 110$ for different grid size calculated in Table 4.9, and from the table we see that the error converges to 10^{-2}.*

Table 4.7, 4.8 and 4.9 shows the option price as compared to the benchmark option price at spot price 90,100 and 110 respectively. From the Tables 4.10, 4.11 and 4.12, the overall relative error of the TPFA method under local volatility is in the order of 10^{-2}.

Consider Figure 4.3 which shows the relative error obtained by different methods from the benchmark results.

Table 4. Problems 2 and 3. Computational time to compute a solution u that has a relative error $< 10^{-4}$ at $t = 0$ and $s = 90, 100, 110$.

	Discrete dividends				Local volatility			
Method	European call		American call		Smooth		Implied	
MC-S	*6.0e + 01	(3)	–		×		×	
QMC-S	1.6e + 00	(4)	–		–		–	
FFT	1.5e − 03	(7)	–		–		–	
FGL	3.6e − 03	(14)	8.1e − 02	(6)	–		–	
COS	8.8e − 04	(5)	2.4e − 03	(4)	1.7e − 02	(4)	–	
FD	2.0e − 02	(4)	1.5e − 02	(4)	2.2e − 02	(4)	1.2e + 00	(4)
FD-NU	1.6e − 02	(4)	1.5e − 02	(4)	3.7e − 02	(4)	8.9e − 01	(4)
FD-AD	2.1e − 02	(4)	2.3e − 02	(5)	3.6e − 02	(4)	8.8e − 01	(4)
RBF	2.3e − 01	(4)	1.1e − 01	(4)	5.5e − 02	(4)	2.4e + 00	(4)
RBF-FD	4.2e − 01	(4)	2.7e + 00	(4)	2.2e + 01	(4)	1.1e + 02	(4)
RBF-PUM	3.3e − 02	(4)	3.0e − 02	(4)	1.4e − 01	(4)	9.0e − 01	(4)
RBF-LSML	5.0e − 01	(4)	1.2e + 00	(4)	1.7e − 01	(4)	4.0e + 00	(4)

Note: The numbers within parentheses indicate the approximate number of correct digits in the result. A ' – ' indicates not implemented, while ' × ' means implemented, but not accurate.

Figure 4.3: *Table of relative error obtained by using different numerical method. Source : (von Sydow et al., 2015).*

From the highlighted column in the Figure 4.3 we see the relative errors obtained using different numerical methods. We know that the relative error obtained by the TPFA method is in the order of 10^{-2} which is in line with that of the finite difference methods (FD, FD-NU and FD-AD) and better than that of the RBF methods. Therefore by taking $N_s \geq 1000$ the TPFA method can yield accurate results.

The codes used in the essay can be accessed in Google colab by clicking on the link provided below:

https://colab.research.google.com/drive/1nIjd5WpGWK_i0MQOFM-1G9RIkXvm_rly?usp=sharing

5. Conclusions

In this essay, we presented the discretization of the Black-Scholes PDE in space and time using TPFA method. The main objective of this essay was the pricing of an European option under local volatility using TPFA method. We compare the results obtained to that of benchmark paper by von Sydow et al. (2015).

For the case of constant volatility, we found that for $N_s \geq 1000$, we achieve a stable value with a relative error of order 10^{-3} which is in line with the best performing results of the benchmark paper.

In the case of local volatility the TPFA method, gives a relative error of 10^{-2} which is again in line with the best performing value of the benchmark paper.

We therefore conclude that the TPFA method is an appropriate method to price an option.

In future work, we will price an option using TPFA method under a more realistic local volatility consistence with market prices.

Acknowledgements

Firstly acknowledge AIMS and its funders for supporting this work, as well as my supervisor, Dr. Hermann Azemtsa Donfack from University of Johannesburg and my co-supervisor Mr. Rock Stephane Koffi from African Institute for Mathematical Sciences (AIMS) for their unwavering encouragement support, and positive criticism which inspired this work.

Thirdly, I want to thank my tutor Dr. Faraniaina Rasolofoson for help and the push she gave me during the course of this work.

Lastly I want to thank my family, friends and AIMS family for the love and support they gave me during this study at AIMS, above all I thank God for the things he has done and still doing in my life.

References

Bjork, T. *Arbitrage Theory in Continuous Time*. Oxford University Press, 3 edition, 2009. URL https://EconPapers.repec.org/RePEc:oxp:obooks:9780199574742.

Black, F. and Scholes, M. *The Pricing of Options and Corporate Liabilities*. The University of Chicago Press, 1973.

Capinski, M. and Zastawniak, T. *Mathematics for Finance: An Introduction to Financial Engineering*. Springer Undergraduate Mathematics Series. Springer London, 2003. ISBN 9781852338466. URL https://books.google.co.za/books?id=4xfyBwAAQBAJ.

Chacha, W. M. *Pricing of a European Call Option Under a Local Volatility Interbank Offered Rate Model*. PhD thesis, JKUAT-PAUSTI, 2018.

Courtadon, G. A more accurate finite difference approximation for the valuation of options. *Journal of Financial and Quantitative Analysis*, pages 697–703, 1982.

Dupire, B. et al. Pricing with a smile. *Risk*, 7(1):18–20, 1994.

Durrett, R. *Probability: Theory and Examples*. Cambridge University Press, 2019.

Fernandes, M. M. *Finite Differences Schemes for Pricing of European and American Options*. Technical University of Lisbon Lisbon, Portugal, 2009.

Haug, E. *The Complete Guide to Option Pricing Formulas*. MacGraw-Hill, 2007.

Hull, J., editor. *Option, Futures, and Other Derivatives*. Number 133 in Finanial Mathematics. Pearson, Providence, RI, 2018.

Hull, J. and White, A. *The Pricing of Option on Asset with Stochastic Volatility*. American Finance Association, 1987.

Kazeem, F. E. Multilevel Monte Carlo Simulation in options pricing. Msc, University of the Western Cape, 2014.

Kloeden, P. E. and Platen, E. Numerical solution of stochastic differential equations. *SIAM Review*, 37:272–275, 06 1995. doi: $10.1137/1037073$.

Koffi, R. S. and Tambue, A. Convergence of the two point flux approximation and a novel fitted two-point flux approximation method for pricing options. *arXiv preprint arXiv:1912.12737*, 2019.

Lanieri, R. *Option theory and Trading*. John Wiley and Son Inc, 2009.

Merton, R. C. Option pricing when underlying stock returns are discontinuous. *Journal of Financial Economics*, 3(1-2):125–144, 1976.

Ramström, A. *Pricing of European and Asian options with Monte Carlo simulations*. Umeå University, 2017.

Roman, S. Introduction to the mathematics of finance. From risk management to options pricing. 07 2020.

Ross, S. M. Chapter 10 - brownian motion and stationary processes. In Ross, S. M., editor, *Introduction to Probability Models (Tenth Edition)*, pages 631 – 666. Academic Press, Boston, tenth edition edition, 2010. ISBN 978-0-12-375686-2. doi: https://doi.org/10.1016/B978-0-12-375686-2.00012-1. URL http://www.sciencedirect.com/science/article/pii/B9780123756862000121.

Shreve, S. E. *Stochastic Calculus for Finance I*. Springer, 2004.

von Sydow, L., Josef Höök, L., Larsson, E., Lindström, E., Milovanović, S., Persson, J., Shcherbakov, V., Shpolyanskiy, Y., Sirén, S., Toivanen, J., et al. Benchop–the benchmarking project in option pricing. *International Journal of Computer Mathematics*, 92(12):2361–2379, 2015.

Wang, S. A novel fitted finite volume method for the black–scholes equation governing option pricing. *IMA Journal of Numerical Analysis*, 24(4):699–720, 2004.

Weijst, R. W. B. V. D. Numerical solutions for the stochastic local volatility model. Msc, Delft University of Technology Faculty Electrical Engineering, Mathematics and Computer Science Delft Institute of Applied Mathematics, 2017.

White, R. Opengamma quantitative research local volatility. OpenGamma Quantitative Research n. 2, 2013.

Wilmott, P. *Paul Wilmott introduces quantitative finance*. John Wiley & Sons, 2007.